

Complex domain wall dynamics in compressively strained $\text{Ga}_{1-x}\text{Mn}_x\text{As}$ epilayers

L. Herrera Diez, R. K. Kremer, A. Enders,* M. Rössle,† E. Arac,‡ J. Honolka,§ and K. Kern
Max-Planck-Institut für Festkörperforschung, Heisenbergstrasse 1, 70569, Stuttgart, Germany

E. Placidi and F. Arciprete
*Dipartimento di Fisica, Università di Roma "Tor Vergata",
and CNR-INFN, Via della Ricerca Scientifica 1, I-00133 Roma, Italy*
(Dated: October 18, 2019)

The domain wall induced reversal dynamics in compressively strained $\text{Ga}_{1-x}\text{Mn}_x\text{As}$ was studied employing the magneto-optical Kerr effect and Kerr microscopy. Due to the influence of an uniaxial part in the in-plane magnetic anisotropy $90^\circ \pm \delta$ domain walls with considerably different dynamic behavior are observed. While the $90^\circ + \delta$ reversal is identified to be propagation dominated with a small number of domain walls, the case of $90^\circ - \delta$ reversal includes the nucleation of many domain walls. The domain wall nucleation/propagation energy ϵ for both transitions are estimated using model calculations from which we conclude that single domain devices can be achievable using the $90^\circ + \delta$ mode.

PACS numbers: 75.50.Pp, 75.60.Ch, 75.60.Jk

The discovery of the ferromagnetic semiconductor $\text{Ga}_{1-x}\text{Mn}_x\text{As}$ and the possible implementation into spintronic devices triggered great interest in understanding its fundamental properties[1]. The linkage between carrier density and magnetic properties in this hole mediated ferromagnet allows tuning of its magnetic properties such as the Curie temperature (T_c) upon changing the carrier concentration [2]. In addition, magnetic domain wall (DW) logic operations may be implemented including magneto-resistive read-outs. However, any application in this direction requires a full control over magnetic reversal dynamics, which in most cases happens via the nucleation and propagation of domain walls. So far, domain wall studies by means of Kerr microscopy (KM) in $\text{Ga}_{1-x}\text{Mn}_x\text{As}$ have been mostly performed in films with tensile strain where the magnetization pointed perpendicular to the plane [3]. $\text{Ga}_{1-x}\text{Mn}_x\text{As}$ with in-plane magnetization has been extensively studied using magneto-transport measurements, however, this techniques does not provide spatially resolved information about DW nucleation and propagation processes. In this study we present the direct observation of DW motion in compressively strained $\text{Ga}_{1-x}\text{Mn}_x\text{As}$ by KM and the dependence of the DW dynamics on the direction of the applied magnetic field. In addition, hysteresis loops have been measured employing the magneto-optical Kerr effect (MOKE). All measurements were done on Hall Bar devices of $150\mu\text{m}$ width, patterned in $[1\bar{1}0]$ and $[110]$ directions using photolithography.

The $\text{Ga}_{1-x}\text{Mn}_x\text{As}$ sample was grown in a RIBER 32 molecular beam epitaxy (MBE) system equipped with a reflection high-energy electron diffraction (RHEED) setup for *in situ* monitoring of the growth. Prior to $\text{Ga}_{1-x}\text{Mn}_x\text{As}$ deposition, a GaAs buffer layer of approximately 400 nm was grown on a Si-doped GaAs(001) substrate ($n \approx 10^{18} \text{ cm}^{-3}$), in As_4 overflow at $\approx 590^\circ\text{C}$, and at a rate of $0.8 \mu\text{m/h}$. After 10 minutes post-growth annealing under As_4 flux, the temperature was lowered to 270°C for $\text{Ga}_{1-x}\text{Mn}_x\text{As}$ deposition. Using an As_4 :Ga flux ratio of 50 a 170 nm $\text{Ga}_{1-x}\text{Mn}_x\text{As}$ layer was grown at a rate of 0.33 ML/sec. During $\text{Ga}_{1-x}\text{Mn}_x\text{As}$ growth a clear two-dimensional (1×2) RHEED pattern was observed with no indication of MnAs precipitates at the surface (no spotty RHEED pattern). Ga, Mn and As_4 fluxes were calibrated by an ion gauge placed in the substrate position (beam equivalent pressure - BEP). A nominal Mn concentration of $x = (2.3 \pm 0.1) \%$ was estimated on the basis of flux (BEP) ratios of As_4 , Ga, and Mn. The high quality of the grown films has also been verified by measuring the X-ray diffraction pattern of the film. Typical diffraction profiles for $\text{Ga}_{1-x}\text{Mn}_x\text{As}/\text{GaAs}$ structures have been found, which contain two distinct peaks around the (004) Bragg reflex corresponding to the GaAs and $\text{Ga}_{1-x}\text{Mn}_x\text{As}$ layers [4].

Longitudinal MOKE measurements have been done at a temperature of $T \sim 3\text{K}$ changing the direction of the in-plane applied field with respect to the $[1\bar{1}0]$ direction in order to map the coercivities and thus the magnetic anisotropy. Along the $[110]$ and $[1\bar{1}0]$ directions only one switching field is observed within the available field range, while in other directions as in the case of the $[100]$ direction (45°), two transitions were found. The polar plot presented in Fig.1 (left) illustrates this behaviour in $\text{Ga}_{1-x}\text{Mn}_x\text{As}$ very similar to what have been found by other authors[5]. In addition, the magnetization value as a function of temperature has been measured with a SQUID magnetometer (Fig.1 (right)). The Curie tem-

*Present address:Department of Physics and Astronomy, University of Nebraska, Lincoln, NE 68588, USA.

†Present address:Department of Physics, University of Fribourg, Chemin du Musée 3, CH-1700 Fribourg, Switzerland.

‡Present address:Forschungszentrum Karlsruhe, Institut für Festkörperphysik, 76021 Karlsruhe, Germany.

§Electronic address: j.honolka@fkf.mpg.de

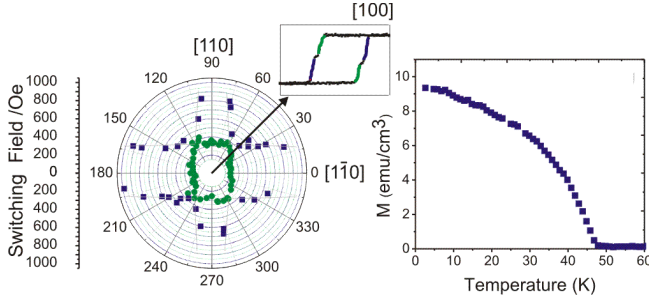


FIG. 1: First (green symbols) and second (blue symbols) switching fields as a function of the direction of the applied field with respect to the $[1\bar{1}0]$ direction measured at $T = 3\text{K}$ (left). A two step hysteresis loop can be seen along $[100]$ (45°). Magnetization as a function of temperature measured at $H = 1\text{ T}$ with SQUID in zero field cooling (right).

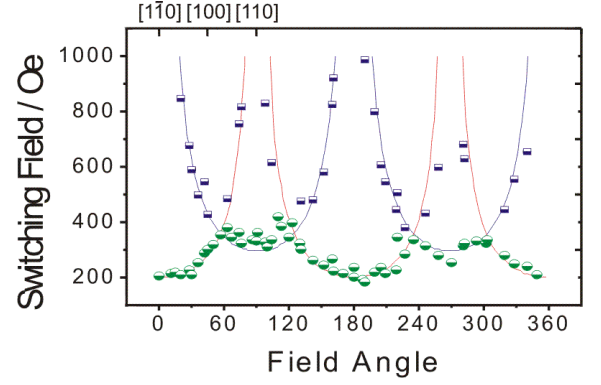


FIG. 3: Fits of the experimental results of Fig.1 (left). The blue and red lines represent fits to Eq. (2) considering $90^\circ + \delta$ and $90^\circ - \delta$ DWs, respectively. The color code is that of Fig.1.

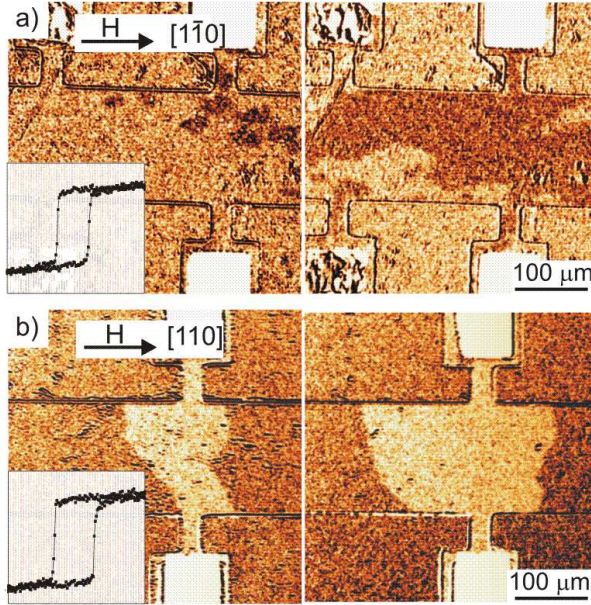


FIG. 2: DW nucleation and propagation for the field applied in the $[1\bar{1}0]$ (a) and $[110]$ (b) directions at two consecutive times. The respective hysteresis loops showing single switching events are displayed as insets. A larger number of domains is found by applying the field along the $[1\bar{1}0]$ direction.

perature and saturation magnetization values determined from this measurement are: $T_c = (48 \pm 2)\text{ K}$ and $M = (9.4 \pm 0.1)\text{ emu/cm}^3$.

Fig.2 shows Kerr images[6] of the domain wall transitions mediating the magnetization reversal for the field applied along the $[1\bar{1}0]$ (a) and $[110]$ (b) directions, respectively. They correspond to hysteresis curves with single switching events as displayed in the insets. The two top and bottom figures were taken at consecutive times. A clear asymmetry in the nucleation behaviour is observed. For the field applied in the $[1\bar{1}0]$ direction (Fig. 2 (a)) the DWs nucleate in a large number of centers. In contrast, when the field is applied in the $[110]$ direction (b) the transition is dominated by the propagation of a

few DWs nucleated at the contact pads.

In the following we will present evidence supporting the existence of two different kind of DWs which seem to be the cause for the asymmetry in the reversal behaviour. These two DW types are given by the interplay of uniaxial and biaxial magnetic anisotropy.

Assuming a fourfold crystalline anisotropy plus an uniaxial contribution the energy of a single domain state can be described by:

$$E = \frac{K_c}{4} \sin^2(2\varphi) + K_u \sin^2(\varphi - 135^\circ) - MH \cos(\varphi - \varphi_H) \quad (1)$$

where K_c and K_u are the biaxial and uniaxial anisotropy constants, M is the magnetization, H the magnetic field, and φ and φ_H are the angles of M and H with the $[100]$ direction. The presence of an uniaxial easy axis along the $[110]$ direction gives a rectangular shape to the first switching field data points in Fig.1 (left) which would otherwise be a square in case of pure biaxial anisotropy. This effect determines the shift of the global easy axes by $\delta/2 = (15 \pm 2)^\circ$ which means that the global easy axes are located $(60 \pm 2)^\circ$ from the $[1\bar{1}0]$ direction and at $(30 \pm 2)^\circ$ from the $[110]$ direction. By equating the DW nucleation/propagation energy ϵ to the Zeeman energy difference between the initial and final states of the magnetization reversal, an expression can be derived which very well reproduces the two branches of the switching field observed in the MOKE measurement (Fig.3) [7] [8]:

$$H_{90 \pm \delta} = \frac{\epsilon_{90 \pm \delta}}{M\sqrt{2} \cos(45 \mp \frac{\delta}{2})(\sin(\varphi_H) \mp \cos(\varphi_H))} \quad (2)$$

The red and blue lines in Fig.3 are obtained by considering $90^\circ - \delta$ and $90^\circ + \delta$ DWs, respectively. Taking this into account, the switching field obtained with field along the $[1\bar{1}0]$ direction would correspond to a 60° DW since it is observed that the experimental value for the switching field lays on the red fit curve. Similarly, for the field applied in the $[110]$ axis, the switching field is found on the blue fit curve and consequently corresponds to a 120° DW. As discussed earlier these two types of DWs

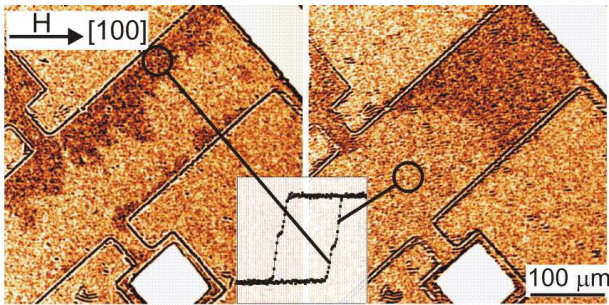


FIG. 4: Kerr images of DWs involved in the first (left) and second (right) switching event for the field applied along the $[100]$ direction. In the MOKE hysteresis loop an intermediate plateau appears between the first and the second switching event (see inset).

seem to show a very different nucleation/propagation behavior.

As indicated in Fig.1 (left), the second transition can not be triggered by applying the field either along the $[1\bar{1}0]$ or the $[110]$ directions within the available magnetic field range. However, to corroborate the observations for the field applied along these two directions, the nucleation has been studied for the field applied in the $[100]$ direction. In this case the longitudinal axis of the Hall Bar was fixed at an angle of 45° with respect to the direction of the field. According to the plot of switching field vs. field angle in Fig.1 (left), in the $[100]$ direction (45°) both of the two transitions can be observed, which add up to a full 180° reorientation. The two switching events are clearly visible in the MOKE signal in the inset of Fig.4. According to the fit in Fig.3, the first switching field along the $[100]$ axis corresponds to a $90^\circ - \delta$ DW transition (60°) and the second to a $90^\circ + \delta$ (120°) DW. In analogy with the previously shown dynamics it is expected that a larger number of nucleation centers for the first switching field (laying on the red line of the fitting curve) and only few domains and a reversal consequently dominated by DW propagation are expected for the second switching field (laying on the blue line of the fitting curve). The results

shown in Fig.4 (left, first transition) and (right, second transition) demonstrate this behaviour and therefore support the notion of the presence of two species of DWs with different dynamics.

From the fitting we extract a ratio of ϵ for the two types of DWs of $(\epsilon_{90+\delta}/\epsilon_{90-\delta}) \approx 2.5$. The experimental results thus imply a considerably lower nucleation/propagation energy for the $90^\circ - \delta$ transition with respect to $90^\circ + \delta$. At the same time KM proves that low ϵ values are correlated with a larger number of nucleation sites. We therefore conclude that the dynamics shifts from a propagation dominated regime to a partly nucleation dominated one for high and low ϵ , respectively. In the former case the observed low number of DWs is determined by single defects within the Hall devices serving as nucleation centers.

In conclusion, extensive MOKE and Kerr-microscopy studies of the nucleation and propagation behavior of DWs in $\text{Ga}_{1-x}\text{Mn}_x\text{As}$ Hall bar devices revealed substantially different dynamics for two observed species of DWs. They correspond to $90^\circ \pm \delta$ DWs and they originate from the uniaxial part of the magnetic anisotropy. While the $90^\circ + \delta$ reversal is found to be propagation dominated with a small number of DWs, the $90^\circ - \delta$ case includes nucleation of many DWs. The measured coercivities for both reversals can be very well fitted by a model which includes the uniaxial anisotropy contribution. From the fits a considerably lower nucleation/propagation energy ϵ for the $90^\circ - \delta$ transition with respect to the $90^\circ + \delta$ transition is derived, which suggests an inverse correlation of ϵ with the number of nucleated DWs. In the case of $90^\circ + \delta$ the observed low number of DWs is determined by few defects within the Hall devices serving as nucleation centers, which opens the possibility to design single DW devices e.g. for magneto-logic elements.

Acknowledgments

We wish to thank Dr. Dinnebier for X-ray diffraction and P. Kopold for TEM measurements.

-
- [1] H. Ohno, *Science* **281**, (1998) 951.
 - [2] T. Dietl, H. Ohno, F. Matsukura, J. Cibert, D. Ferrand, *Science* **287**, (2000) 1019.
 - [3] M. Yamanouchi, D. Chiba, F. Matsukura, H. Ohno, *Nature* **428**, (2004) 539.
 - [4] J. Sadowski, J. Z. Domagala, J. Bak-Misiuk, S. Kolesnik, M. Sawicki, K. Świątek, J. Kanski, L. Ilver, V. Strom, *J. Vac. Sci. Technol. B* **18**, (2000) 1697.
 - [5] H. Tang, R. Kawakami, D. Awschalom, M. Roukes, *Phys.*

- Rev. Lett.* **90**, (2003) 107201.
- [6] I. Horcas, R. Fernández, J. M. Gómez-Rodríguez, J. Colchero, *Rev. Sci. Instrum.* **78**, (2007) 013705.
- [7] K. Pappert, C. Gould, M. Sawicki, J. Wenisch, K. Brunner, G. Schmidt, L. W. Molenkamp, *New J. Phys.* **9**, (2007) 354.
- [8] R. P. Cowburn, S. Gray, J. Ferré, J. Bland, J. Miltat, *J. Appl. Phys.* **78**, (1995) 7210.